ChemPhysChem

Research Article
doi.org/10.1002/cphc.202400681

Chemistry Europe
European Chemical Societies Publishing

www.chemphyschem.org

Ab Initio Simulation of Raman Fingerprints of Sulfur/Carbon Copolymer Cathodes During Discharge of Li–S Batteries

Rana Kiani,[a] Huiying Sheng,[b, c] Timo Held,[a] Oliver Löhmann,[b] Sebastian Risse,[b] Daniel Sebastiani,[a] and Pouya Partovi-Azar*[a]

Sulfur/carbon copolymers have emerged as promising alternatives for conventional crystalline sulfur cathodes for lithium-sulfur batteries. Among these, sulfur-*n*-1,3-diisopropenylbenzene (S/DIB) copolymers, which present a 3D network of DIB molecules interconnected via sulfur chains, have particularly shown a good performance and, therefore, have been under intensive experimental and theoretical investigations. However, their structural complexity and flexibility have hindered a clear understanding of their structural evolution during redox reactions at an atomistic level. Here, by performing state-of-the-art *ab initio* molecular dynamics-based Raman spectroscopy simulations, we investigate the spectral fingerprints of S/DIB copolymers arising from local structures during consecutive reactions with lithium. We discuss in detail Raman spectral changes in particular frequency ranges which are common in S/DIB copolymers having short sulfur chains and those consisting of longer ones. We also highlight those distinctive spectroscopic fingerprints specific to local S/DIB structures containing only short or long sulfur chains. This distinction could serve to help distinguish between them experimentally during discharge. Our theoretically predicted results are in a good agreement with experimental Raman measurements on coin cells at different discharge stages. This work represents, for the first time, an attempt to compute Raman fingerprints of sulfur/carbon copolymer cathodes during battery operation including quantum-chemical and finite-temperature effects, and provides a guideline for Raman spectral changes of arbitrary electrodes during discharge.

Introduction

The remarkable theoretical specific capacity of elemental sulfur (~1675 mA h/g), its eco-friendly nature, and its abundance make lithium-sulfur (Li–S) batteries an attractive alternative to current lithium-ion batteries.[1,2] Nevertheless, their cycle life has so far been limited due to certain drawbacks. A notable challenge is the formation of long-chain, soluble lithium poly-sulfides during the discharge and their shuttling through the conventional electrolytes,[3,4] which leads to a depletion of the active material and formation of an insulating layer around the anode. All these processes result in an irreversible capacity fade in Li–S batteries.[5–8] To tackle these issues, numerous studies have focused on structural optimization of sulfur cathodes including utilization of sulfur/carbon copolymers. In order to synthesize S/C copolymers, many researchers have employed the inverse vulcanization reaction as a facile synthesis method which provides a straightforward way for controlling sulfur content. Among others, sulfur-*n*-1,3-diisopropenylbenzene (S/DIB) copolymer has shown a promising performance as an active cathode material for Li–S batteries.[9,10]

Structural characterization of S/DIB copolymers has been the subject of several studies so far.[10–13] For example, similar to other S/C copolymers involving sulfur chains,[14–20] thermodynamically preferred S/DIB structures consist of short S_n chains, n~4.[12] The shorter sulfur chains are expected to result in a hindrance in the formation of higher-order Li-poly-sulfides and consequently a stable cycling of 1500 cycles has been reported.[21] Despite qualitative descriptions of the discharge mechanism of S/DIB copolymer cathodes,[10,21] an atomistic view on their structural evolution during the lithiation reactions is still lacking. Such an insight can lead to morphology optimization of sulfur/carbon copolymers toward more efficient cathodes.

In this study, we aim to address the structural evolution of S/DIB copolymers during discharge by performing finite-temperature Raman spectroscopy simulations, combining quantum-chemical calculations with *ab initio* molecular dynamics simulations on model S/DIB systems. Here, we study the lithiation reactions of DIB–S_n–DIB with two different sulfur chain lengths, namely $n = 4$ and 8, and focus on Raman spectroscopic fingerprints of the final structures at different stages of

[a] R. Kiani, T. Held, Prof. Dr. D. Sebastiani, Dr. P. Partovi-Azar
Institute of Chemistry, Martin Luther University Halle-Wittenberg, Von-Danckelmann-Platz 4, 06120 Halle (Saale), Germany
E-mail: pouya.partovi-azar@chemie.uni-halle.de

[b] H. Sheng, Dr. O. Löhmann, Dr. S. Risse
Department for Electrochemical Energy Storage, Helmholtz-Zentrum Berlin für Materialien und Energie, Hahn-Meitner-Platz 1, 14109 Berlin, Germany

[c] H. Sheng
Department of Chemistry, Humboldt Universität zu Berlin, Brook-Taylor-Str. 2, 12489 Berlin, Germany

Supporting information for this article is available on the WWW under https://doi.org/10.1002/cphc.202400681

discharge. The huge computational effort of such an investigation is substantially reduced by the efficient Wannier polarizability method for the estimation of the dynamics of polarizability tensors during *ab initio* molecular dynamics simulations,[22–25] fully bypassing the time-consuming linear response calculations. We demonstrate common spectroscopic trends occurring during discharge of Li–S batteries based on S/DIB copolymer cathodes involving both short and long sulfur chains. Moreover, we predict spectroscopic fingerprints during discharge specific to the copolymers having short sulfur chains or those consisting of long ones. Our theoretical predictions are validated against Raman spectroscopy measurements on coin cells at different discharge states. These findings serve as an important step towards simulation of contributions from the local copolymer cathode structures to the Raman spectrum during discharge and will contribute to the advancement of material analysis and, thereby, can lead to an enhanced performance of Li–S batteries.

Computational Details

We consider DIB–S_n–DIB as target molecules in vacuum as a local structure of poly(sulfur-*n*-1,3-diisopropenylbenzene), where $n = 4$ and 8, representing local structures of the S/DIB copolymers consisting of short and long sulfur chains, respectively. In S/DIB copolymers, the terminal sulfur atoms forming C–S bonds are usually referred to as organic sulfur atoms. The C–S bonds remain stable during reactions with lithium,[10] resulting in lithium-saturated chains where the number of lithium atoms reacting with the sulfur chain is twice the number of sulfur atoms minus two. Therefore, consecutive lithiation reactions of S/DIB copolymers are described here by:

$$\begin{aligned} &\mathrm{DIB-S}_n\mathrm{-DIB} + m\,\mathrm{Li}^+ + m\,\mathrm{e}^- \rightarrow \\ &\mathrm{DIB-Li}_m\mathrm{S}_n\mathrm{-DIB},\ m = 2, 4, \ldots, 2n-2 \end{aligned} \quad (1)$$

In our computations, we treat the Li^+ and e^- pair as a single lithium atom. The initial structures are prepared by adding Li atoms along the S chain at distinct positions. These structures then go through atomic coordinate optimizations. In total, about 360 optimizations are carried out. At each lithiation step, the lowest-energy product structure is considered as a candidate for the actual lithiation product. As indicated in Eq. (1), we continue with sequential lithiation reactions until the saturation of the sulfur chain with lithium atoms is achieved. For simplicity, we specifically consider even numbers of lithium atoms in each reaction.

All coordinate optimizations are performed at density-functional theory (DFT) level using the CP2K/QUICKSTEP software package[26] in conjunction with a DZVP-MOLOPT basis set,[27] as well as Perdew–Burke–Ernzerhof (PBE)[28] exchange-correlation energy functional and Geodecker Teter-Hutter (GTH) pseudopotentials.[29,30] The semi-empirical DFT-D3[31] method is also used to correct for the long-range dispersion interactions.

After identifying the minimum-energy structure at each lithiation step, we study its structural stability by carrying out a 20 ps DFT-based *ab initio* molecular dynamics (AIMD) simulation in the canonical ensemble (NVT), specifically a canonical sampling through velocity rescaling (CSVR) thermostat[32] with a time constant of 10.0 fs, at an elevated temperature of 500 K. In rare cases where an unexplored structure is formed at the elevated temperature, new geometry optimization is performed and the energy is compared to the previously found product structure at the corresponding lithiation step. In a following step, another round of AIMD simulations is performed on the structurally stable products for 20 ps in the NVT ensemble to achieve equilibrium at 300 K. This is followed by 20 ps of AIMD simulations in the micro-canonical ensemble (NVE) to sample the polarizabilities needed for the simulation of Raman spectra. A time step of 1 fs is used in the AIMD simulations, while the polarizabilities are sampled every 5 fs. The AIMD simulations are also performed using the CP2K software with the same simulation setup as mentioned earlier.

The Raman spectroscopy simulations are performed using the efficient Wannier polarizability method.[22–25] This method allows for a very efficient estimation of the dynamics of the polarizability, which can be about 1000 times faster compared to the conventional approaches, for example those based on linear response theory.[25] Such an efficiency can allow for performing *ab initio* Raman spectroscopy simulations on many intermediate electrode structures during battery operation.

The interaction energies are corrected for the basis set superposition error based on the counterpoise correction of Boys and Bernardi.[33]

In a lithium-sulfur battery sporting an S/DIB copolymer as cathode, reactions occur at the interface between the electrolyte and the three dimensional network of the copolymer. As such, only those local S/DIB structures are exposed to the electrolyte which happen to be on the surface. Therefore, adding a solvent to the molecular systems considered here for the local structures, where the solvent fully surrounds the molecules, might not be fully realistic. Nevertheless, we check the effect of solvent around Li-Saturated DIB–Li_6S_4–DIB using an implicit solvent model.[34] We find that the change in the bond lengths remain below 3% (please see the Supplementary Information). Moreover, as will be discussed later, the agreement between the calculated and experimental spectra is found to be remarkable. This ensures that, although the effect of the electrolyte cannot be completely neglected, in the frequency range of sulfur activity (below 1100 cm^{-1}), the observed Raman peaks and their evolution mostly arise from the Li–S structures which emerge during discharge. Therefore, all calculations in this work are performed in vacuum.

Results and Discussion

During structure optimizations and AIMD simulations at 500 K and 300 K, we do not observe any C–S bond breaking, irrespective of the sulfur chain length and the depth of discharge. However, we see a gradual breaking of S–S bonds in the course of discharge. This implies that the organic sulfur atoms play an important role in keeping the emerging lithium-sulfur structures connected to the organic groups via C–S bonds. This has also been argued earlier to be one of the factors contributing to the good electrochemical performance of S/DIB copolymers by anchoring the emerging lithium-sulfur structures to the organic groups.[10] In fact, here we find the interaction energies between the lithium-sulfur structures and the organic groups (DIB molecules together with organic sulfur atoms) at 100% depth of discharge to be about 1.4 times as high as a typical C–S covalent bond ($E_{C\text{-}S}$ ~7.2 eV)[35] both in DIB–Li_6S_4–DIB and DIB–$Li_{14}S_8$–DIB.

Calculated room-temperature *ab initio* Raman spectra of DIB–S_4–DIB and DIB–S_8–DIB molecules at different stages of discharge are shown in Figures 1 and 2, respectively. The corresponding lithiated structures are also shown in the insets. By decomposing the total Raman spectra into local contributions,[23–25] we find that among all Raman activities spanning 0–3300 cm^{-1} range, the signals in 0–1200 cm^{-1} predominantly arise from the emerging lithium-sulfur structure between two DIB molecules [Figure 1(a), panel (IV) and Figure 2(a), panel (VIII)]. The observed signals in the higher frequency range (1200–3300 cm^{-1}) mostly correspond to vibrations of the DIB molecules (see Figure S1 in the Supplementary

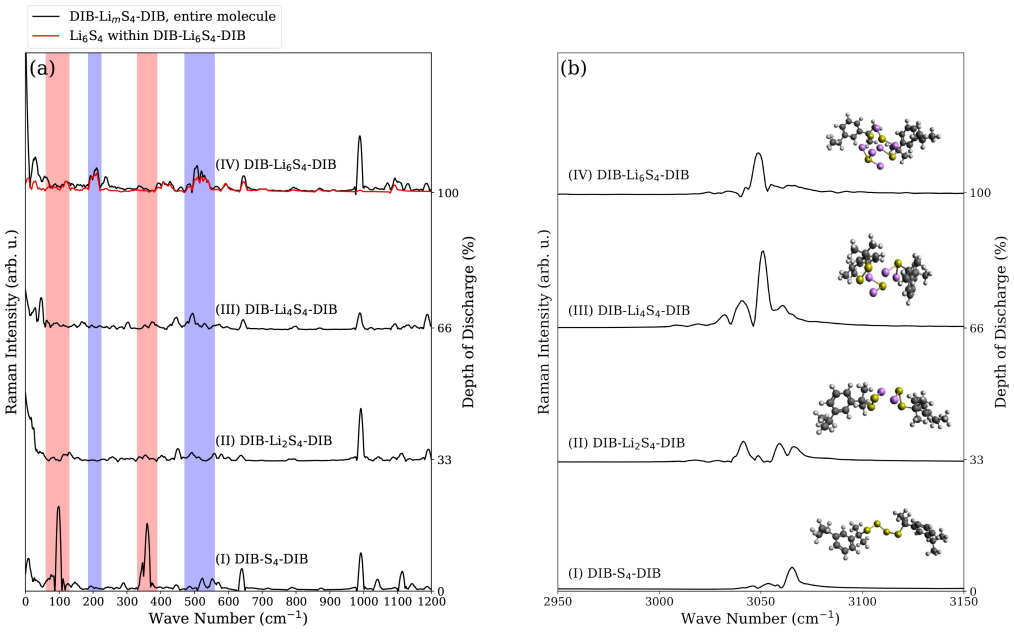

Figure 1. Computed Raman spectra for (I) DIB–S_4–DIB, (II) DIB–Li_2S_4–DIB, (III) DIB–Li_4S_4–DIB, and (IV) DIB–Li_6S_4–DIB molecules in vacuum. (a) Spectra in the range of 0–1200 cm^{-1} and (b) Spectra in the range of 2950–3150 cm^{-1}. The black curves represent the computed Raman spectra of the entire DIB–Li_mS_4–DIB molecule, while the red curve represents the partial Raman spectra of Li_6S_4 within the DIB–Li_6S_4–DIB molecule. The intensities in 2950–3150 cm^{-1} in (b) are multiplied by a factor of ten for clasity. The purple, yellow, black, and white colors in the atomic structures indicate lithium, sulfur, carbon, and hydrogen atoms, respectively.

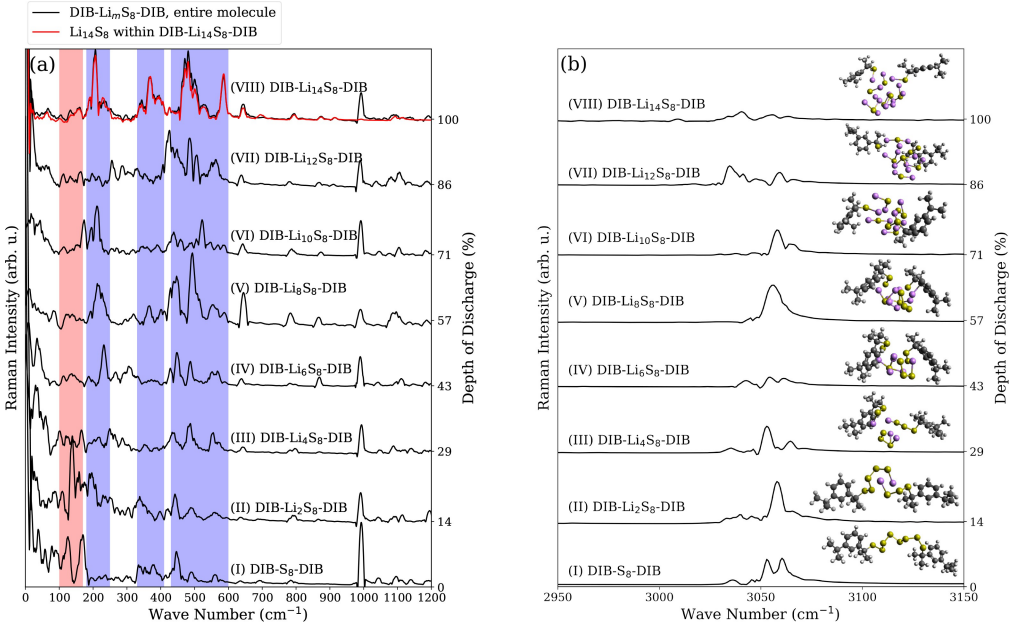

Figure 2. Computed Raman spectra for (I) DIB–S_8–DIB, (II) DIB–Li_2S_8–DIB, (III) DIB–Li_4S_8–DIB, (IV) DIB–Li_6S_8–DIB, (V) DIB–Li_8S_8–DIB, (VI) DIB–$Li_{10}S_8$–DIB, (VII) DIB–$Li_{12}S_8$–DIB, and (VIII) DIB–$Li_{14}S_8$–DIB molecules in vacuum. (a) Spectra in the range of 0–1200 cm^{-1} and (b) Spectra in the range of 2950–3150 cm^{-1}. The black curves represent the computed Raman spectra of the entire DIB–Li_mS_8–DIB molecule, while the red curve represents the partial Raman spectra of $Li_{14}S_8$ within DIB–$Li_{14}S_8$–DIB molecule. The intensities in (b) are multiplied by a factor of ten for clarity. The atomic colouring scheme is the same as Figure 1.

Information). Here, we particularly focus on the activities arising from lithium-sulfur structures.

Short Sulfur Chains

The Raman spectra obtained for the DIB–S_4–DIB structure [Figure 1(a), panel (I)] agrees well with earlier investigations.[13] The activities observed at around 100 cm^{-1} and 350 cm^{-1} in Figure 1(a), panel (I), are attributed to S_4 chain deformations in the DIB–S_4–DIB structure. However, as seen in Figure 1(a), these activities become unnoticeable upon reaction with lithium due to the breaking of S–S bonds along the chain. Based on our observation, as the copolymer is discharged to around 33% [Figure 1(a), panel (II)], the S_4 chain splits at the mid-bond, resulting in the formation of two shorter S_2 chains. As the lithiation continues, another sulfur bond is broken [Figure 1(a), panel (III)]. The same pattern is observed until the final lithiation stage, where no S–S covalent bond is present anymore [Figure 1(a), panel (IV)]. Additionally, the lithiation reactions appear to be reversible. The reversibility of the reactions is particularly checked by removing two lithium atoms from the optimized DIB–Li_4S_4–DIB structure [Figure 1(a), panel (III)] followed by an atomic coordinate optimization on the resulting structure. We observe a restoration of a broken S–S bond leading to a DIB–Li_2S_4–DIB structure, similar to the one shown in Figure 1(a), panel (II).

At 100% depth of discharge, where the system contains the highest possible number of lithium atoms, a notable Raman activity is observed around 200 cm^{-1}, as shown in Figure 1(a), panel (IV). This activity can be attributed to the lithium-sulfur structure.[36]

Moreover, in agreement with previous studies[23] where the Raman activities in the range of 350–500 cm^{-1} have predominantly been attributed to lithium-sulfur structure, our results reveal a gradual increase in Raman activities within the 400–500 cm^{-1} range as more lithium atoms react with sulfur [Figure 1(a)]. In the range of 480–580 cm^{-1}, specifically at 520 cm^{-1}, a broad Raman activity is observed as the depth of discharge reaches 100%, which should also arise from the formation of the lithium-sulfur structure.[36]

Based on partial Raman analysis, the activity at ~575 cm^{-1} can be assigned to the C–S bond stretching [see Figure S5 in the Supplementary Information].[13] In agreement with our observation, it has been shown before[21] that this peak gets slightly blue-shifted during the discharge.

The activity in about 650, 710, 790, 870, and 900 cm^{-1} Raman shifts can be due to collective Raman-active vibrations of lithium-sulfur structures and the DIB groups. These vibrations are observed in all lithiated samples of DIB–S_4–DIB and DIB–S_8–DIB. This also holds for the activities seen around 1100 cm^{-1} (see Figure 1(a), panel (IV) and the Supplementary Information).

The vibrational mode around 1000 cm^{-1} is a strong indicator of a benzene ring breathing vibration in all systems. Here, we observe that the intensity of this mode fluctuates non-monotonically with the depth of discharge. As will be discussed later, the intensity of this band could be heavily affected by the presence of binder material and/or carbon black.

Furthermore, we observe that the formation of lithium-sulfur structures could have a far-reaching effect. For example, as shown in Figure 1(b), we see that the frequency range attributed to the C–H stretching vibrations becomes broader as a function of the depth of discharge. For clarity, the intensities are scaled up ten times compared to Figure 1(a). A redshift is seen in the frequency of the dominant peak at ~3065 cm^{-1} [Figure 1(b), panel (I)] towards ~3048 cm^{-1} [Figure 1(b), panel (IV)] in the course of discharge. The decomposition of the spectra reveals that the observed redshift corresponds to the weakening of the C–H bonds proximal to the lithiation center (see Figure S2 in the Supplementary Information).

Long Sulfur Chains

The calculated Raman spectra of a DIB–Li_mS_8–DIB molecule at different stages of discharge are presented in Figure 2(a), panels (I)–(VIII). The Raman spectrum of DIB–S_8–DIB structure [Figure 2(a), panel (I)] agrees well with our previous investigations on S/DIB copolymers with long sulfur chains.[13] In the range of 100–180 cm^{-1}, two prominent peaks are observed. In our previous study, these activities in copolymers with longer sulfur chains have been attributed to sulfur chain deformation and S–S–S bending, and they gradually decline with increasing weight percentage of DIB.

At a discharge state of approximately 14% [Figure 2(a), panel (II)], we observe a structure with one broken S–S bond, resulting in two shorter chains, namely S_3 and S_5. As lithiation continues, an additional sulfur bond is broken [Figure 2(a), panel (III)]. Similar to the case of DIB–S_4–DIB, this pattern continues during further lithiations up to the final stage of discharge, where there is no S–S covalent bond remaining in DIB–$Li_{14}S_8$–DIB [Figure 2(a), panel (VIII)]. Here, we also observe that S–S bond breaking can be reversible as well.

Upon splitting of the S_8 chain in DIB–S_8–DIB at early stages of discharge [Figure 2(a), panel (II)], we observe rather intensive Raman activities in the range of 100–250 cm^{-1}, resembling those previously observed in free (isolated) S_4 and S_8 chains.[13] This shows that the S/DIB copolymer cathode should involve quasi-free S chains at low depths of discharge. Here, these activities are attributed to S–S–S bending within the S_5 unit of DIB–Li_2S_8–DIB (see Figures S3 and S4 in the Supplementary Information for further details).

As the system gets further lithiated, a significant Raman activity is observed at around 200 cm^{-1} [Figure 2(a), panels (II)–(VIII)]. Similar to the case of DIB–Li_mS_4–DIB [Figure 1(a)], this activity can generally be assigned to the emerging lithium-sulfur structure.

Similarly, Raman activities in the 320–400 and 420–600 cm^{-1} ranges arise from the lithium-sulfur structure. These activities become more noticeable with the increasing number of lithium atoms. At 100% depth of discharge [Figure 2(a), panel (VIII)], the dominant Raman activity in 320–400 cm^{-1} range coincides with the characteristic Raman activity of Li_2S solid.[37]

The Raman activity around 450 cm^{-1} predominantly originates from S–S stretching vibration in longer sulfur chains. As previously discussed,[13] this activity is a key factor in distinguishing between long and short sulfur chains. The activity at ~450 cm^{-1} is found to be absent at 100% depth of discharge as there is no S–S covalent bond present in the DIB–$Li_{14}S_4$–DIB molecule anymore. Instead, a broad activity emerges at 100% depth of discharge at 470–550 cm^{-1} which seems to come almost entirely from the formed lithium-sulfur structure [see the red curve in Figure 2(a), panel (VIII)]. However, our analysis based on the partial Raman spectrum of the S_8 chain within DIB–S_8–DIB shows that the activity at ~480 cm^{-1} should partially arise from the DIB molecules as well. It is worth noting that this activity arising from the organic molecules should be present at all stages of discharge.

Similar to the case of DIB–S_4–DIB, the activity at ~575 cm^{-1} can be attributed to the C–S bond stretching [see Figure S5 in the Supplementary Information].[13] In qualitative agreement with previous studies,[21] this peak undergoes a blueshift from ~575 cm^{-1} to ~585 cm^{-1} during discharge.

The activity in the 600–900 cm^{-1} range can also be attributed to collective Raman-active vibrations of sulfur (either lithiated or otherwise) and the organic groups. As in the case of DIB–S_4–DIB, the activities seen around 1100 cm^{-1} should also arise from similar coupled Li–S/DIB vibrations (see the Supplementary Information).

We also observe a similar behavior in the C–H stretching frequency range as in DIB–S_4–DIB. As shown in Figure 2(b), the frequency range associated with C–H stretching bandwidth broadens with increasing depth of discharge. However, in the case of DIB–S_8–DIB, no meaningful frequency shift is observed. Figure 3 illustrates how the C–H stretching bandwidth increases during the discharge process for both sulfur chain lengths (S_4 and S_8). This broadening indicates that the introduction of lithium into the system and hence its interaction with sulfur atoms affects C–H bonds vibrations, resulting in nonidentical oscillators (see Figure S2 in the Supplementary Information for partial Raman analysis).

Comparing panel (IV) in Figure 1(a) with panel (VIII) in Figure 2(a), we observe that S/DIB copolymers containing short chains and those having long ones show similar Raman features at 100% depth of discharge. The main difference is that the bands are broader in the case of DIB–S_8–DIB. This is due to the fact that in lithiated DIB–S_8–DIB structure, the number of nonidentical oscillators with Raman activities at certain frequency ranges are higher than that in the DIB–S_4–DIB system in the same frequency ranges. However, the Raman activity at ~450 cm^{-1} corresponding to the S–S stretching mode could still serve as a fingerprint for distinguishing between local copolymer structures consisting of short and those having long sulfur chains. Although the corresponding band shows an insignificant intensity at 0% depth of discharge in DIB–S_4–DIB [Figure 1(a), panel (I)], it exhibits an intensive band in DIB–S_8–DIB from 0% up to 86% depth of discharge [Figure 2(a), panels (I)-(VII)]. At 100% depth of discharge, where no S–S covalent bond is present, the intensity of this band becomes negligibly small in both DIB–Li_6S_4–DIB and DIB–$Li_{14}S_8$–DIB structures. In addition to this band, the Raman activities at ~200 cm^{-1} during discharge can also be used to distinguish between short and long sulfur chains. While the band at ~200 cm^{-1} only appears at fully discharged DIB–S_4–DIB [Figure 1(a)], our results show a rather intensive activity in 200–250 cm^{-1} range at 14% to 100% depth of discharge of DIB–S_8–DIB [Figure 2(a), panels (II)–(VI)].

Comparison with Raman Measurements

Figure 4 shows the *ex situ* measured Raman spectra of the synthesized SDIB10 sample which corresponds to an average sulfur chain length of 22 sulfur atoms. All the intensities are normalized with respect to the carbon D band at ~1350 cm^{-1}. The spectra are obtained at different depths of discharge, namely 0% (black), 66% (red), and 100% (blue). Despite differing sulfur chain lengths, these spectra can be qualitatively compared with those presented in Figure 2(a) for DIB–S_8–DIB. It is worth noting that apart from activities coming from the S/DIB copolymer, those from the electrolyte, carbon black, and binder material are also present in the experimental spectra.

Although the relative intensities in the spectrum corresponding to 0% depth of discharge in Figure 4 (black curve) do not fully match with those in panel (I) of Figure 2(a), the peak positions agree well. As discussed earlier, the activity at around 200 cm^{-1} in Figure 4 should come from sulfur chain deforma-

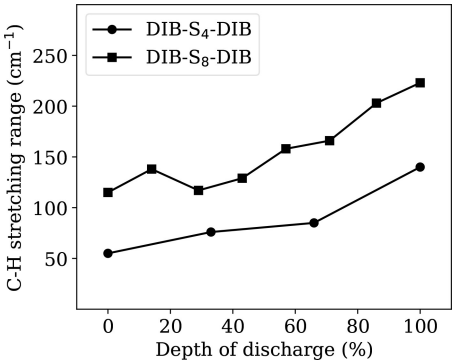

Figure 3. C–H stretching bandwidth as a function of depth of discharge for DIB–S_4–DIB (circles) and DIB–S_8–DIB (squares).

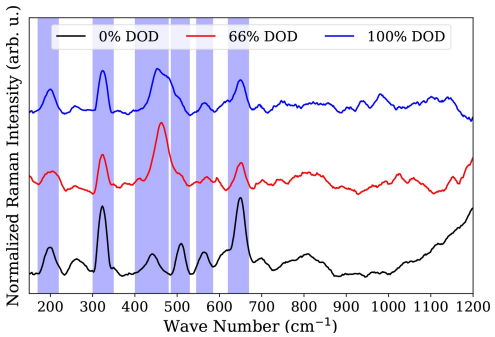

Figure 4. Experimental Raman measurement on SDIB10. DOD stands for depth of discharge.

tion at early stages of discharge. The collective vibrations in the lithium-sulfur structure toward the end of discharge also have an activity around the same frequency. The activity in 300–400 cm^{-1} in the black curve in Figure 4 (0% depth of discharge) can also be attributed to sulfur chain deformation, as has been revealed in our previous study.[13] This activity, similar to the one at ~200 cm^{-1} also arises from lithium-sulfur vibrations at higher depths of discharge [Figure 2(a), panel (VIII)]. As discussed earlier, the activity at ~450 cm^{-1} can be assigned to S–S stretching, the one at ~500 cm^{-1} to DIB vibrations, ~560 cm^{-1} to C–S stretching, and finally those at ~650 cm^{-1} to coupled (lithium-) sulfur/DIB vibrations. These assignments can be further justified based on the fact that, for example, the peak at ~450 cm^{-1} is found to become unnoticeable at 100% depth of discharge (blue curve), while the ones at ~500 cm^{-1}, ~560 cm^{-1}, and ~650 cm^{-1} are found at all stages of discharge. A clear broad activity is observed in Figure 4 in 450–500 cm^{-1} range. Our calculations show that this broad activity arises mostly from the emerging lithium-sulfur structure and is found to occur in a comparable frequency range, namely 470–550 cm^{-1}.

It should be noted here that although the spectral fingerprints of the local structures and their evolution during discharge are well predicted in our calculations, an *in situ/operando* Raman spectrum of a realistic S/DIB copolymer cathode should, in general, be calculated by adding the local contributions weighted by their formation energies.[12,19] However, as demonstrated here, the spectral evolution of the cathode during discharge occurs at around the same frequencies, namely ~200 cm^{-1}, 300–400 cm^{-1}, and ~450 cm^{-1}, irrespective of the sulfur chain length in the local structures. The same behavior could be expected in local S/DIB structures containing intermediate sulfur chain lengths. Therefore, the cathode contribution to the Raman spectrum in the frequency range of sulfur activity computed through the weighted sum of local contributions should appear approximately similar to any individual contribution.

Conclusions

In summary, we have investigated the spectral evolution of sulfur/1,3-diisopropenylbenzene (S/DIB) copolymers as a function of depth of discharge by performing *ab initio* finite-temperature Raman spectroscopy simulations. The focus has been set on the spectroscopic fingerprints arising from local S/DIB structures containing low and high sulfur content, corresponding to short and long sulfur chains, respectively. This study, represents an important step toward quantum-chemical simulation of Raman spectroscopy based on *ab initio* molecular dynamics simulations on battery electrodes during operation. This has been facilitated by using the Wannier polarizability method[22–25] to efficiently estimate the polarizability dynamics in many intermediate lithiated structures.

Our current study dives deeper into understanding of the complex discharge mechanism of S/DIB copolymer cathodes. We have observed that local S/DIB structures containing short and those consisting of long sulfur chains show similar Raman features at 100% depth of discharge. However, we have found frequency ranges in which short- and long-sulfur chain containing local structures have distinctive Raman activities during discharge. For example, the Raman activity at ~450 cm^{-1} (S–S stretching) can serve as a fingerprint for distinguishing between local copolymer structures consisting of short and those having long sulfur chains. Although the corresponding band shows an insignificant intensity at early to mid stages of discharge in structures with short sulfur chains, it shows an intensive band from 0% up to 86% depth of discharge in those containing long sulfur chains. At 100% depth of discharge, where no S–S covalent bond is present, the intensity of this band can become negligibly small irrespective of the sulfur chain length in the local copolymer structure. In addition to this, the Raman activities at ~200 cm^{-1} during the discharge can also be used to distinguish between short and long sulfur chains. The band at ~200 cm^{-1} only appears at fully lithiated local S/DIB structures with short sulfur chains. However, we have found a rather intensive activity in 200–250 cm^{-1} range from 14% to 100% depth of discharge of those local copolymer structures consisting of long sulfur chains. These theoretical predictions have been validated against *ex situ* Raman measurements on S/DIB cathodes at different stages of discharge and provide practical insights into designing and characterizing sulfur/carbon copolymers cathode materials.

Experimental

Materials and Synthesis

Chemicals

All reagents, namely sulfur (≥99.5%, Sigma–Aldrich), 1,3-diisopropenylbenzene (DIB, 97%, TCI), sodium carboxymethyl cellulose (CMC, MW 250,000, Sigma–Aldrich), polyacrylic acid (PAA, MW 450,000, Sigma–Aldrich), electrolyte (purchased from E-lyte) consisting of lithium bis(trifluoromethane)sulfonimide and 2 wt% lithium nitrate in a 1:1 *v/v* mixture of 1,3-dioxolane and 1,2-dimethoxy ethane, metallic lithium chips (99.95%, China Energy Lithium), polypropylene separator (Celgard-2700), and carbon black (super p, Macklin) are used directly.

Synthesis of SDIB10

SDIB10 is synthesized using the previously reported method.[10,11,13,38] 10 wt% sulfur is added into a glass vial equipped with a magnetic stir bar and heated to 130 °C in a thermostated oil bath. DIB is added to the fully molten sulfur using a syringe and stirred for 10 minutes to achieve a homogeneous mixture.

SDIB10 Cathode Preparation

The synthesized S/DIB is further heated to 185 °C for 8–10 minutes, which results in vitrification of the mixture. The product is then cooled down to room temperature. The obtained product is mixed with carbon black and a binder mixture of CMC/PAA (1/1 *w/w*) in a mass ratio of 75:20:5 in water. The slurry is then ball milled and blade cast onto carbon coated aluminum foil. The areal mass

loading of sulfur inside the electrode is around 3 mg/cm^2. After getting completely dried, the prepared electrode is cut into disks with 12 mm diameters to be used as cathode in a coin cell.

Instrumentation and Measurements

The prepared cathodes are assembled into CR2032 coin cells with electrolyte, a polypropylene separator, and a lithium foil anode in an argon filled glove box. Cells are tested in a VMP3 potentiostat from 0.8–3.0 V at 0.1 C for 4 cycles. A renishaw QONTOR instrument with a 532 nm laser is employed for the *ex situ* Raman spectroscopy in the range from 0–4000 cm^{-1} with a resampling interval of 1 cm^{-1}. Cycled cathodes at 0%, 66%, and 100% depth of discharge and a cathode without cycling are measured.

Acknowledgements

The authors gratefully acknowledge DFG funding via projects PA3141/3 (Project number 420536636), PA3141/5 (Project number 446879138), and SPP 2248 "Polymer-based Batteries". Additionally, H. S. kindly acknowledges the financial support from the China Scholarship Council (No. 202308080034). The computations have been mostly performed on a Bull Cluster at the Center for Information Services and High Performance Computing (ZIH) at TU Dresden via the project 'p_oligothiophenes'. Open Access funding enabled and organized by Projekt DEAL.

Conflict of Interests

The authors declare no conflict of interest.

Data Availability Statement

The data that support the findings of this study are available from the corresponding author upon reasonable request.

Keywords: Li–S battery · sulfur/carbon copolymer · Raman spectroscopy · density functional theory · ab initio molecular dynamics

[1] M. Winter, R. J. Brodd, *Chem. Rev.* **2004**, *104*, 4245.
[2] P. G. Bruce, *Solid State Ionics* **2008**, *179*, 752.
[3] X. Liang, C. Hart, Q. Pang, A. Garsuch, T. Weiss, L. F. Nazar, *Nat. Commun.* **2015**, *6*, 5682.
[4] Z. W. Seh, Y. Sun, Q. Zhang, Y. Cui, *Chem. Soc. Rev.* **2016**, *45*, 5605.
[5] S. Evers, L. F. Nazar, *Acc. Chem. Res.* **2013**, *46*, 1135.
[6] X. Ji, L. F. Nazar, *J. Mater. Chem.* **2010**, *20*, 9821.
[7] T. Li, Y. Yu, M. Pei, *J. Phys. Chem. C* **2023**, *127*, 6271.
[8] T. Li, J. Zhang, R. Ren, Y. Tian, *J. Energy Storage* **2024**, *88*, 111600.
[9] A. G. Simmonds, J. J. Griebel, J. Park, K. R. Kim, W. J. Chung, V. P. Oleshko, J. Kim, E. T. Kim, R. S. Glass, C. L. Soles, et al., *ACS Macro Lett.* **2014**, *3*, 229.
[10] A. Hoefling, D. T. Nguyen, P. Partovi-Azar, D. Sebastiani, P. Theato, S.-W. Song, Y. J. Lee, *Chem. Mater.* **2018**, *30*, 2915.
[11] W. J. Chung, J. J. Griebel, E. T. Kim, H. Yoon, A. G. Simmonds, H. J. Ji, P. T. Dirlam, R. S. Glass, J. J. Wie, N. A. Nguyen, et al., *Nat. Chem.* **2013**, *5*, 518.
[12] R. Kiani, D. Sebastiani, P. Partovi-Azar, *ChemPhysChem* **2022**, *23*, e202100519.
[13] R. Kiani, M. Steimecke, M. Alqaisi, M. Bron, D. Sebastiani, P. Partovi-Azar, *RSC Adv.* **2023**, *13*, 27756.
[14] Y. Schütze, R. de Oliveira Silva, J. Ning, J. Rappich, Y. Lu, V. G. Ruiz, A. Bande, J. Dzubiella, *Phys. Chem. Chem. Phys.* **2021**, *23*, 26709.
[15] Y. Schütze, D. Gayen, K. Palczynski, R. de Oliveira Silva, Y. Lu, M. Tovar, P. Partovi-Azar, A. Bande, J. Dzubiella, *ACS Nano* **2023**, *17*, 7889, 10.1021/acsnano.3c01523.
[16] R. Zou, W. Liu, F. Ran, *InfoMat* **2022**, page e12319.
[17] S. Park, S.-J. Kim, Y.-E. Sung, K. Char, J. G. Son, *ACS Appl. Mater. Interfaces* **2019**, *11*, 45785.
[18] P. Partovi-Azar, S. P. Jand, P. Kaghazchi, *Phys. Rev. Appl.* **2018**, *9*, 014012.
[19] P. Partovi-Azar, *Phys. Rev. Appl.* **2022**, *18*, 044072.
[20] C.-J. Huang, J.-H. Cheng, W.-N. Su, P. Partovi-Azar, L.-Y. Kuo, M.-C. Tsai, M.-H. Lin, S. P. Jand, T.-S. Chan, N.-L. Wu, et al., *J. Power Sources* **2021**, *492*, 229508.
[21] A. Rafie, R. Pereira, A. A. Shamsabadi, V. Kalra, *J. Phys. Chem. C* **2022**, *126*, 12327.
[22] P. Partovi-Azar, T. D. Kühne, *J. Comput. Chem.* **2015**, *36*, 2188.
[23] P. Partovi-Azar, T. D. Kühne, P. Kaghazchi, *Phys. Chem. Chem. Phys.* **2015**, *17*, 22009.
[24] P. Partovi-Azar, T. D. Kühne, *Micromachines* **2021**, *12*, 1212.
[25] P. Partovi-Azar, *Phys. Rev. B* **2023**, *108*, 235157.
[26] T. D. Kühne, M. Iannuzzi, M. Del Ben, V. V. Rybkin, P. Seewald, F. Stein, T. Laino, R. Z. Khaliullin, O. Schütt, F. Schiffmann, et al., *J. Chem. Phys.* **2020**, *152*, 194103.
[27] J. VandeVondele, J. Hutter, *J. Chem. Phys.* **2007**, *127*, 114105.
[28] J. P. Perdew, K. Burke, M. Ernzerhof, *Phys. Rev. Lett.* **1996**, *77*, 3865.
[29] S. Goedecker, M. Teter, J. Hutter, *Phys. Rev. B* **1996**, *54*, 1703.
[30] M. Krack, *Theor. Chem. Acc.* **2005**, *114*, 145.
[31] S. Grimme, J. Antony, S. Ehrlich, H. Krieg, *J. Chem. Phys.* **2010**, *132*, 154104.
[32] G. Bussi, D. Donadio, M. Parrinello, *J. Chem. Phys.* **2007**, *126*, 014101.
[33] S. F. Boys, F. Bernardi, *Mol. Phys.* **1970**, *19*, 553.
[34] O. Andreussi, I. Dabo, N. Marzari, *J. Chem. Phys.* **2012**, *136*, 064102.
[35] J. A. Kerr, *Chem. Rev.* **1966**, *66*, 465.
[36] S. Lang, S.-H. Yu, X. Feng, M. R. Krumov, H. D. Abruña, *Nat. Commun.* **2022**, *13*, 4811.
[37] Z. Lin, Z. Liu, N. J. Dudney, C. Liang, *ACS Nano* **2013**, *7*, 2829.
[38] A. J. Berndt, J. Hwang, M. D. Islam, A. Sihn, A. M. Urbas, Z. Ku, S. J. Lee, D. A. Czaplewski, M. Dong, Q. Shao, et al., *Polymer* **2019**, *176*, 118.

Manuscript received: June 28, 2024
Revised manuscript received: October 25, 2024
Accepted manuscript online: October 28, 2024
Version of record online: November 21, 2024